Fluctuation-dissipation relation and stationary distribution for an exactly solvable many-particle model far from equilibrium

Roland R. Netz
Fachbereich Physik, Freie Universität Berlin, 14195 Berlin, Germany
(Dated: December 7, 2017)

An exactly solvable, Hamiltonian-based model of many massive particles that are coupled by harmonic potentials and driven by stochastic non-equilibrium forces is introduced. The stationary distribution as well as the fluctuation-dissipation relation are derived in closed form for the general non-equilibrium case. Deviations from equilibrium are on one hand characterized by the difference of the obtained stationary distribution from the Boltzmann distribution, which is possible because the model derives from a particle Hamiltonian. The difference between the obtained non-equilibrium fluctuation-dissipation relation and the standard equilibrium fluctuation-dissipation theorem allows to quantify non-equilibrium in an alternative fashion. Both indicators of non-equilibrium behavior, i.e. deviations from the Boltzmann distribution and deviations from the equilibrium fluctuation-dissipation theorem, can be expressed in terms of a single non-equilibrium parameter α that involves the ratio of friction coefficients and random force strengths. The concept of a non-equilibrium effective temperature, which can be defined by the relation between fluctuations and the dissipation, is by comparison with the exactly derived stationary distribution shown not to hold, even if the effective temperature is made frequency dependent. The analysis is not confined to close-to-equilibrium situations but rather is exact and thus holds for arbitrarily large deviations from equilibrium. Also, the suggested harmonic model can be obtained from non-linear mechanical network systems by an expansion in terms of suitably chosen deviatory coordinates, the obtained results should thus be quite general. This is demonstrated by comparison of the derived non-equilibrium fluctuation dissipation relation with experimental data on actin networks that are driven out of equilibrium by energy-consuming protein motors. The comparison is excellent and allows to extract the non-equilibrium parameter α from experimental spectral response and fluctuation data.

Systems that are maintained far from equilibrium are interesting for two reasons: First, nature is not in equilibrium, but rather energy is constantly injected and removed through a cascade of interwoven dissipation levels from astrophysical, geophysical down to biological and microbiological length and time scales. Equilibrium theories, that are commonly used to describe natural processes, thus typically employ idealizations and simplifications. Secondly, most theoretical models and principles exclusively apply to equilibrium systems, while methods for the description of non-equilibrium system are less developed, so the study of non-equilibrium phenomena most likely will produce new basic concepts and fundamental insights [1, 2].

There are two distinct ways of characterizing non-equilibrium system: On the one hand, systems far from equilibrium deviate from the Boltzmann distribution, the founding principle of statistical mechanics. Even phase transitions have been observed as a function of the rate at which energy is injected into a system. Examples include phase separation of particles driven by external [3–8] or internal forces [9–14], and the collective response of pedestrians to spatial confinement[15]. Experimentally, symmetry-breaking transitions in suspensions of swimming bacteria and filament systems driven by motor proteins have indeed been demonstrated [16, 17]. Non-equilibrium shape transformations have been described for polymers driven by externally applied torques [18, 19]. For some systems, such effects can be derived by a solution of the governing dynamic equations or by the system's tendency to maximize its dissipation, i.e., its entropy production[20], but a general understanding of non-equilibrium systems based on distribution function theory is missing.

A fundamentally different indicator of non-equilibrium is a violation of the fluctuation-dissipation theorem (FDT), the key theoretical concept to describe dynamics close to equilibrium. According to the FDT, the time derivative of the autocorrelation function of an observable that is coupled to an externally applied time-dependent force is proportional to the linear response function. Modified versions of the FDT that account for non-equilibrium effects have been discussed in the context of laser [21], chaotic [22], glassy [23], colloidal [24] and sheared systems [25, 26]. Generalized non-equilibrium fluctuation-dissipation relations were derived [21, 27–30] and compared with experimental data for glasses [31], colloids [32, 33] and bundles of biological filaments [34, 35].

These two distinct ways of characterizing non-equilibrium systems, i.e. deviations from the Boltzmann distribution and the breakdown of the FDT, could not be compared to each other in the past, simply because of the lack of a suitable model system. The man insight in this paper is derived from an in-depth comparison of these complementary definitions of non-equilibrium for an explicitly solvable particle-based model. In fact, driven non-equilibrium systems pose a number of fundamen-

tal questions: What is the relation between FDT violation and deviations from the Boltzmann distribution, are these two indicators of non-equilibrium behavior necessarily coupled or could – alternatively – only one of them be observed? Why is FDT violation in experimental system, such as biopolymer networks that are driven by protein motors [36], typically seen at low frequencies, is this a property of the active noise spectrum or rather of the biopolymeric network? Can a non-equilibrium system be described by an effective non-equilibrium temperature, which would preserve the symmetry of the Boltzmann distribution and the structure of the FDT (possibly by introducing a frequency-dependent temperature [22, 23])?

What is needed in order to address these questions is a Hamiltonian-based model that is simple enough to allow for in-depth analysis of the distribution functions, yet complex enough to yield non-trivial response functions, and that can be continuously moved away from equilibrium by a suitable control parameter. We here introduce such a model, which consists of n massive active particles that are elastically coupled to a central particle, as schematically depicted in Fig. 1. Each particle is coupled to a heat sink via friction and subject to a stochastic force that drives the system away from equilibrium.

Our theoretical model is motivated by the experimental system of an actin network in the presence of myosin motor proteins, for which a stark FDT violation has been demonstrated at increased ATP concentration [36]. The FDT has been explicitly checked by simultaneously measuring the spatial autocorrelation of a colloidal bead and the response of the bead to an externally applied force [37, 38]. In the absence of motor activity the FDT was demonstrated to be perfectly obeyed, for ATP-induced motor activity the FDT was significantly violated at low frequencies, where the bead fluctuations were seen to be much larger than the bead response [36]. In our comparison with the experimental data, the central particle represents the colloidal probe, while the active particles are the protein motors that are mechanically coupled to the central particle by actin filaments.

Similar models have been studied before in the classical [23, 28, 39] and quantum [40] equilibrium cases in order to understand how friction and memory effects arise from coupled many-particle systems. The main advantage of our non-equilibrium model is that on the one hand the stationary distribution can be calculated explicitly by a mapping on the Fokker-Planck equation, and on the other hand the response and autocorrelation functions can be obtained from the conjugated generalized Langevin equation. We show that a non-Boltzmann stationary distribution and FDT violation occur hand in hand and are described by a single parameter which quantifies departure from equilibrium, denoted as α. We derive the non-equilibrium FDT which allows quantitative description of the experimental frequency-dependent motion of a tracer bead in an ATP driven actin network

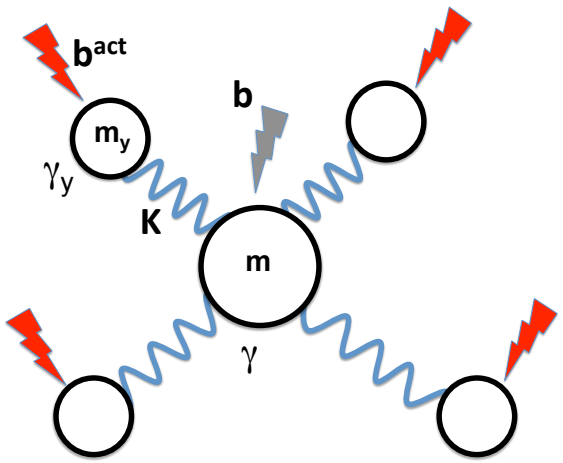

FIG. 1. In the model based on the Hamiltonian Eq. (1), n particles of mass m_y and with a friction coefficient γ_y are elastically coupled to a central particle that has mass m and a friction coefficient γ. The harmonic springs have a strength of K. The n peripheral particles are subject to random forces of strength $b^{\rm act}$ which are tuned to induce non-equilibrium behavior, the central particle is subject to a random force of strength b.

[36]. By the mapping of our model on the experimental spectral data [36] we extract for the non-equilibrium parameter the value $\alpha = 20$, which we interpret in terms of physical parameters such as friction coefficients, particle masses and the input power of motor units. The high value of α indicates that the experimental system is far from equilibrium. Our results do not support the concept of a non-equilibrium effective temperature, rather, non-equilibrium breaks the symmetry of the stationary distribution, vividly demonstrated by couplings between particle velocities and positions, which in equilibrium are absent.

The main strength of our harmonic model is that, due to its simple nature, it allows to derive the stationary distribution and the fluctuation-dissipation relation in an exact manner, that means, arbitrarily far away from equilibrium. Clearly, a harmonic model can always be obtained from a more complex, non-linear mechanical network by a Gaussian expansion in terms of suitably defined deviatory coordinates. Our model should thus quite generally describe mechanical systems far from equilibrium, as long as the mechanical response is close to linear, even when the system is far from equilibrium as described by our non-equilibrium parameter α. This expectation is confirmed by the good comparison of our model with experimental spectral data for driven actin biopolymeric networks.

STATIONARY DISTRIBUTION OF MANY-PARTICLE MODEL

To proceed, we consider a tracer particle of mass m that is via harmonic bonds of strength K coupled to n active particles of mass m_y. The Hamiltonian is given by

$$H = \frac{K_x}{2}x^2 + \frac{m}{2}v^2 + \sum_{i=1}^{n}\frac{K}{2}(x-y_i)^2 + \sum_{i=1}^{n}\frac{m_y}{2}w_i^2, \quad (1)$$

where x and v are the position and the velocity of the tracer bead while y_i and w_i are the positions and velocities of the active particles. The central particle is in addition confined by a harmonic potential of strength K_x. Our one-dimensional model can be trivially generalized to three dimensions. By adding friction terms and random forces to the Hamilton equations, which mimics the presence of a heat bath, we obtain the coupled set of linear Langevin equations

$$\begin{aligned}
\dot{x}(t) &= v(t)\\
m\,\dot{v}(t) &= -\gamma v(t) - (nK+K_x)x(t) + K\sum_i y_i(t) + bF_v(t)\\
\dot{y}_i(t) &= w_i(t)\\
m_y\,\dot{w}_i(t) &= -\gamma_y w_i(t) - K\,(y_i(t)-x(t)) + b_i^{\rm act}F_i^{\rm act}(t), \quad (2)
\end{aligned}$$

where γ is the friction coefficient of the tracer bead and γ_y is the friction coefficient of the active particles. For simplicity, we assume Gaussian random forces with zero mean and and variances $\langle F_v(t)F_v(t')\rangle = 2\delta(t-t')$ and $\langle F_i^{\rm act}(t)F_j^{\rm act}(t')\rangle = 2\delta_{ij}\delta(t-t')$, the random force strengths are b for the tracer bead and $b_i^{\rm act}$ for the active particles. Note that for an equilibrium system one would now fix the noise strengths at values $b^2 = k_BT\gamma$ for the tracer bead and $(b_i^{\rm act})^2 = k_BT\gamma_y$ for the active particles in order to recover Maxwell-Boltzmann distributions for the velocities [41]. We do not do this, but rather analyze the model for arbitrary random force strength distributions. Summing over the equations for the active particles we arrive at the reduced Langevin equations

$$\begin{aligned}
\dot{x}(t) &= v(t)\\
m\,\dot{v}(t) &= -\gamma v(t) - K_x x(t) + nK(y(t)-x(t)) + bF_v(t)\\
\dot{y}(t) &= w(t)\\
m_y\,\dot{w}(t) &= -\gamma_y w(t) - K\,(y(t)-x(t)) + b_yF_w(t) \quad (3)
\end{aligned}$$

where we defined the mean position and velocity of the active particles as $y(t) = \sum_i y_i(t)/n$ and $w(t) = \sum_i w_i(t)/n$. The random force acting on the mean position of the active particles is given by

$$F_w(t) = \sum_{i=1}^{n}\frac{b_i^{\rm act}F_i^{\rm act}(t)}{nb_y} \quad (4)$$

with $b_y^2 = \sum_i (b_i^{\rm act})^2/n^2$ and satisfies $\langle F_w(t)F_w(t')\rangle = 2\delta(t-t')$. The set of linear stochastic differential equations defined by Eq. (3) can be written as a matrix equation

$$\dot{z}_k(t) = -A_{km}z_m(t) + \Phi_{km}F_m(t), \quad (5)$$

where we defined the state vector $\vec{z}(t) = (x(t), v(t), y(t), w(t))$ and the random field vector $\vec{F}(t) = (F_x(t), F_v(t), F_y(t), F_w(t))$. Note that doubly appearing indices are summed over. The matrices appearing in Eq. (5) are given explicitly by

$$A = \begin{pmatrix} 0 & -1 & 0 & 0\\ nK/m + K_x/m & \gamma/m & -nK/m & 0\\ 0 & 0 & 0 & -1\\ -K/m_y & 0 & K/m_y & \gamma_y/m_y \end{pmatrix} \quad (6)$$

and

$$\Phi = \begin{pmatrix} 0 & 0 & 0 & 0\\ 0 & b/m & 0 & 0\\ 0 & 0 & 0 & 0\\ 0 & 0 & 0 & b_y/m_y \end{pmatrix}. \quad (7)$$

The associated Fokker-Planck equation for the time-dependent density distribution $P(\vec{z},t) = P(x,v,y,w,t)$ follows via Kramers-Moyal expansion of Eq. (5) as [41]

$$\dot{P}(\vec{z},t) = \left[\nabla_k A_{km}z_m + \nabla_k\nabla_m C_{km}\right]P(\vec{z},t) \quad (8)$$

where $C_{ij} = \Phi_{ik}\Phi_{jk}$. With the Gaussian Ansatz for the stationary distribution

$$P_0(\vec{z}) = \mathcal{N}^{-1}\exp(-z_iE_{ij}^{-1}z_j/2), \quad (9)$$

where $\mathcal{N}$ is an unimportant normalization constant, we obtain from Eq. (8) and the stationarity condition $\dot{P}(\vec{z},t) = 0$ the equation

$$A_{ii} - A_{ij}z_jE_{ik}^{-1}z_k + C_{ij}(E_{ik}^{-1}z_kE_{jl}^{-1}z_l - E_{ij}^{-1}) = 0. \quad (10)$$

This is equivalent to the Lyapunov equation

$$A_{ik}E_{kj} + A_{jk}E_{ki} = 2C_{ij}, \quad (11)$$

as shown in Supplementary Information (SI), where we also present the explicit solution for all entries of the covariance matrix E_{ij}, which is easily found by solving the set of linear equation defined by Eq. (11). Here we simply note that $E_{xv} = \langle xv\rangle = 0$ and $E_{yw} = \langle yw\rangle = 0$ and that $\langle xw\rangle = -\langle yv\rangle$, which reduces the number of independent covariances from ten (for a symmetric four by four matrix) down to seven. For the remaining seven covariances a fundamental symmetry transpires: if the noise strengths acting on the active and tracer particles, b_y and b, respectively, obey the relation

$$b_y^2 = b^2\gamma_y/(n\gamma), \quad (12)$$

we obtain as stationary solution the simple result

$$P_0 \simeq \exp(-\gamma H/b^2), \quad (13)$$

where H is the Hamiltonian defined in Eq. (1). Thus, ordinary Boltzmann statistics is recovered if the noise strength acting on the tracer particle is given by $b^2 = \gamma k_{\rm B}T$, in which one obtains $P_0 \simeq \exp(-H/k_BT)$. If Eq. (12) holds, we explicitly find $\langle v^2\rangle = k_{\rm B}T/m$, $\langle w^2\rangle = k_{\rm B}T/(nm_y)$, $\langle x^2\rangle = k_{\rm B}T/K_x$ and $\langle (x-y)^2\rangle = k_{\rm B}T/(nK)$ and $\langle xw\rangle = \langle yv\rangle = \langle vw\rangle = 0$. This is precisely what one would derive from standard equilibrium statistical mechanics. To quantify the departure from equilibrium, we define the non-equilibrium parameter α as

$$b_y^2 = (1+\alpha)b^2\gamma_y/(n\gamma). \tag{14}$$

For $\alpha = 0$ we recover Eq. (12) and thus the equilibrium stationary distribution. For $\alpha \neq 0$ we obtain a non-equilibrium stationary distribution that is characterized by non-vanishing couplings between velocities and positions $\langle xw\rangle = -\langle yv\rangle \neq 0$ as well as $\langle vw\rangle \neq 0$, and positional covariances that deviate from the equilibrium solution. The complete and exact stationary non-equilibrium solution is shown in the SI, due to the length of the resulting expressions we exemplarily show here only the tracer-bead positional variance in the vanishing mass (i.e. overdamped) limit $m = m_y = 0$,

$$\langle x^2\rangle = \frac{k_{\rm B}T}{K_x}\left(1 + \frac{\alpha n\gamma_y}{n\gamma_y + \gamma + \gamma_y K_x/K}\right). \tag{15}$$

The following properties are noteworthy: i) For $\alpha = 0$ the second term vanishes and thus the equilibrium result for the mean-square displacement of a particle in a harmonic potential of strength K_x, the first term, is recovered. ii) For active particles into which the random forces inject more energy than in equilibrium, i.e. for $\alpha > 0$, the tracer particle is less confined and its variance goes up, this effect is linear in the number n of coupled active particles and linear in α. iii) Although it is vital to consider the complete Fokker-Planck equation with finite particle masses, since this allows to observe the symmetry breaking of the stationary distribution for $\alpha \neq 0$ in terms of velocity-position correlations very clearly, non-equilibrium effects survive in the over damped, mass-less limit. iv) In the absence of elastic coupling between tracer and active particles, i.e. for $K = 0$, the non-equilibrium effect (not surprisingly) vanishes. v) The non-equilibrium effect also vanishes if the active particles have no friction, for $\gamma_y = 0$. vi) Finally, for vanishing confinement potential of the tracer particle, i.e. for $K_x = 0$, the variance is infinity regardless of α, we thus see that active particles cannot confine a particle that in equilibrium is unconfined (which is a consequence of spatial homogeneity).

We conclude this section by saying that non-equilibrium in our model is quantified by a single parameter α, defined in Eq. (14), which depends on the ratio of friction coefficients and noise strengths acting on the particles. For $\alpha \neq 0$ a symmetry-breaking transition of the stationary solution and a departure from the equilibrium Boltzmann distribution is obtained. We can straightforwardly recognize the non-equilibrium nature of the distribution for $\alpha \neq 0$, because our model is based on a Hamiltonian and thus the equilibrium distribution is directly given by the Boltzmann weight Eq. (13). This is a significant advantage of our approach that is Hamiltonian based, compared to alternative approaches that start from a dynamic evolution equation.

NON-EQUILIBRIUM FLUCTUATION-DISSIPATION RELATION

We now connect to the experimentally observed FDT violation. For this we need to calculate autocorrelation functions and response functions, this is most conveniently done using the Langevin equation derived earlier. For simplicity, and in order to cast our results for the tracer-bead motion in the form of a generalized Langevin equation, we set the active particle mass to zero, $m_y = 0$. We have seen that this does not eliminate non-equilibrium effects, as the particle positions deviate from Boltzmann distribution also in the overdamped case, as demonstrated in Eq. (15).

The explicit solution of the Langevin equation (3) for the active particle motion, described by the variable $y(t)$, for $m_y = 0$ reads

$$y(t) = \int_{-\infty}^{t} {\rm d}t' {\rm e}^{-(t-t')K/\gamma_y}\left[\frac{K}{\gamma_y}x(t') + \frac{b_y}{\gamma_y}F_w(t')\right]. \tag{16}$$

Inserting this solution into the Langevin equation (3) for the tracer particle, described by the variables $x(t)$ and $v(t)$, we obtain the generalized Langevin equation

$$m\dot{v}(t) = -K_x x(t) - \int_{-\infty}^{\infty} {\rm d}t' \Gamma(t-t')v(t) + F(t) + F_{\rm ext}(t), \tag{17}$$

where $F_{\rm ext}(t)$ is an external force which we added for later derivation of the response function. The memory function that appears in Eq. (17) is given by

$$\Gamma(t) = \theta(t)\left[2\gamma\delta(t) + nK{\rm e}^{-tK/\gamma_y}\right] \tag{18}$$

where $\theta(t)$ denotes the Theta function with the properties $\theta(t) = 1$ for $t > 0$ and $\theta(t) = 0$ for $t < 0$, which makes the memory function obviously single-sided. The noise $F(t)$ in Eq. (17) is given by

$$F(t) = bF_v(t) + \frac{nKb_y}{\gamma_y}\int_{-\infty}^{t} {\rm d}t' {\rm e}^{-(t-t')K/\gamma_y}F_w(t') \tag{19}$$

and consists of the noise acting directly on the tracer particles (proportional to b) and a term due to noise acting on the active particles (proportional to b_y). The latter term consists of a convolution integral because this noise

is transmitted via the elastic linkers of strength K. Defining the auto-correlation function of the random noise as $C_{\rm FF}(t) = \langle F(0)F(t)\rangle$ we obtain

$$C_{\rm FF}(t) = k_{\rm B}T\left[2\gamma\delta(t) + n(1+\alpha)K{\rm e}^{-|t|K/\gamma_y}\right]. \quad (20)$$

Comparing Eq. (18) and Eq. (20) we see that $C_{\rm FF}(t) = k_{\rm B}T\Gamma(|t|)$, a consequence of the standard fluctuation-dissipation theorem [41], only holds for $\alpha = 0$, for $\alpha \neq 0$ the two functions differ, which points to FDT violation. The memory function $\Gamma(t)$ and the random-force autocorrelation function $C_{\rm FF}(t)$ are not directly measurable, in order to connect to experiments we need to calculate response functions and particle positional autocorrelation functions. The response function $\chi(t)$ is defined via the particle positional response to an externally applied force $x(t) = \int_{-\infty}^{\infty} {\rm d}t'\chi(t-t')F_{\rm ext}(t')$, where causality demands $\chi(t) = 0$ for $t < 0$. From the Fourier-transformed generalized Langevin equation (17)

$$\tilde{x}(\omega) = \int {\rm d}t{\rm e}^{-i\omega t}x(t) = \tilde{\chi}(\omega)\left[\tilde{F}(\omega) + \tilde{F}_{\rm ext}(\omega)\right] \quad (21)$$

we obtain, by averaging over the noise, $\langle\tilde{x}(\omega)\rangle = \tilde{\chi}(\omega)\tilde{F}_{\rm ext}(\omega)$ and therefore the response function

$$\tilde{\chi}(\omega) = \frac{\langle\tilde{x}(\omega)\rangle}{\tilde{F}_{\rm ext}(\omega)} = \left[K_x - \omega^2 m + i\omega\tilde{\Gamma}(\omega)\right]^{-1}. \quad (22)$$

The Fourier-transform of the positional autocorrelation function $C_{\rm xx}(t) = \langle x(0)x(t)\rangle$ is from Eq. (21) and setting the external force to zero given by

$$\tilde{C}_{\rm xx}(\omega) = \tilde{C}_{\rm FF}(\omega)\tilde{\chi}(\omega)\tilde{\chi}(-\omega). \quad (23)$$

The equilibrium FDT reads in the time domain $\chi(t) = -\theta(t)\dot{C}_{\rm xx}(t)/(k_{\rm B}T)$, from which we obtain via Fourier-transform the standard result for the imaginary part of the response function [41]

$$\tilde{\chi}^I(\omega) = -\omega\tilde{C}_{\rm xx}(\omega)/(2k_{\rm B}T). \quad (24)$$

From Eq. (22) we see that

$$\tilde{\chi}^I(\omega) = -\omega\tilde{\Gamma}^R(\omega)\tilde{\chi}(\omega)\tilde{\chi}(-\omega). \quad (25)$$

From Eqs. (23) and (25) we obtain that

$$\frac{-\omega\tilde{C}_{\rm xx}(\omega)/(2k_{\rm B}T)}{\tilde{\chi}^I(\omega)} = \frac{\tilde{C}_{\rm FF}(\omega)/(2k_{\rm B}T)}{\tilde{\Gamma}^R(\omega)} = 1 + \Xi(\omega) \quad (26)$$

where in the last step we introduced the spectral function $\Xi(\omega)$ that quantifies deviations from the standard FDT shown in Eq. (24). Equation (26) corresponds to the generalized, exact FDT and is valid arbitrarily far away from equilibrium. The Fourier-transformed real part of the memory kernel and random force autocorrelation function follow from Eqs. (18) and (20) as

$$\tilde{\Gamma}^R(\omega) = \gamma + \frac{n\gamma_y}{1+\omega^2\gamma_y^2/K^2} \quad (27)$$

and

$$\tilde{C}_{\rm FF}(\omega)/(2k_{\rm B}T) = \gamma + \frac{n(1+\alpha)\gamma_y}{1+\omega^2\gamma_y^2/K^2}. \quad (28)$$

By inserting these expressions into the generalized FDT in Eq. (26), we finally obtain for $\Xi(\omega)$ the explicit result

$$\Xi(\omega) = \frac{\alpha n\gamma_y}{n\gamma_y + \gamma + \gamma\gamma_y^2\omega^2/K^2} \simeq \frac{\alpha}{1+\tau^2\omega^2} \quad (29)$$

where in the last step we made the approximate assumption that $n\gamma_y > \gamma$, which means that the friction coefficient of the active particles γ_y (which includes half of the physical linker molecule connecting active particles to the tracer bead) times the number of active particles n is larger than the friction coefficient γ of the tracer particle, which is certainly a sensible limit to take. Interestingly, the final result for $\Xi(\omega)$ is not proportional to the number of active particles n, this result can be traced back to our model assumption that the noise acting on different active particles is uncorrelated. The relaxation time defined in Eq. (29) is given by

$$\tau^2 = \frac{\gamma_y\gamma}{nK^2}. \quad (30)$$

We see that the final expression for the non-equilibrium FDT correction term $\Xi(\omega)$ is of a surprisingly simple Lorentz form and in fact linearly proportional to the non-equilibrium coefficient α. This allows for direct comparison with experiments and in particular to extract α as well as τ from experimental data. In Fig. 2 we compare $\Xi(\omega)$, defined in Eq. (26) and calculated from experimental data for $\tilde{C}_{\rm xx}(\omega)$ and $\tilde{\chi}^I(\omega)$ obtained for actin networks with added myosin motors in the presence of ATP (red data points) [36], with the Lorentz scaling form in Eq. (29) (red line). The general agreement between the experimental data and the predicted functional form of $\Xi(\omega)$ is very good, the extracted fitting parameters are $\alpha = 20$ for the non-equilibrium parameter and $\tau = 1s$ for the relaxation time scale. The blue data are obtained in the absence of ATP and closely agree with the expected result $\Xi(\omega) = 0$ (black horizontal line). The large fit result for α shows that the experimental system is far from equilibrium and thus a non-perturbative treatment of non-equilibrium effects, as accomplished in our calculation, is needed; the value of the relaxation time τ will be interpreted in the Discussion.

DISCUSSION

By the comparison with experimental data in Fig. 2 we see that the derived generalized FDT Eq. (26) works well even for complex active biological systems. The advantage of our model is that all terms have physical meaning.

To demonstrate this, we first connect the non-equilibrium parameter α to the injected power due to

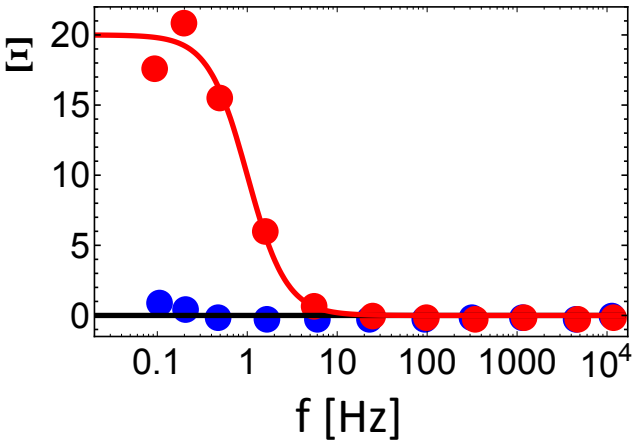

FIG. 2. The spectral function $\Xi(\omega)$ plotted here as a function of frequency $f = \omega/(2\pi)$ characterizes deviations from the equilibrium fluctuation-dissipation theorem and is defined in Eq. 26. Experimental data from motor-protein driven actin networks in the presence of ATP (red circles) [36] are compared with the prediction Eq. 29 (red line), the extracted non-equilibrium parameter is $\alpha = 20$ and the time scale is $\tau = 1s$. Blue circles denote experimental results in the absence of ATP [36] and agree with the expected equilibrium limit $\Xi(\omega) = 0$ (black horizontal line).

active particles. For this we consider the Langevin equation for a single active particle in the absence of coupling to the tracer particle (i.e. for $K = 0$), which follows from Eq. (2) as

$$m_y\, \ddot{y}_i(t) = -\gamma_y \dot{y}_i(t) + b_i^{\rm act} F_i^{\rm act}(t). \qquad (31)$$

Multiplying by $\dot{y}_i(t)$ and averaging we obtain

$$\frac{d}{dt}\langle \frac{m_y}{2} \dot{y}_i^2 \rangle = 0 = -\gamma_y \langle \dot{y}_i^2 \rangle + b_i^{\rm act} \langle \dot{y}_i F_i^{\rm act} \rangle. \qquad (32)$$

The left side is the time derivative of the average kinetic energy of the particle, the right side is the difference of the dissipation rate $I = \gamma_y \langle \dot{y}_i^2 \rangle$ and the injected power $P = b_i^{\rm act} \langle \dot{y}_i F_i^{\rm act} \rangle$. In a stationary state, the injected power is equal to the dissipation rate and we have $P = I$. We explicitly obtain for the dissipation rate (see SI)

$$I = \gamma_y \langle \dot{y}_i^2 \rangle = \frac{(1+\alpha) k_B T \gamma_y}{m_y} \qquad (33)$$

which contains an equilibrium dissipation (independent of α) and a non-equilibrium part proportional to α. We see that both finite mass m_y and finite friction coefficient γ_y are needed in order to make a meaningful comparison of the non-equilibrium parameter α and the dissipation rate I. For the mass of the active particle we assume $m_y = 4\pi R^3 \rho/3$ with water density $\rho = 10^3 kg/m^3$ and for the friction coefficient we take the Stokes expression $\gamma_y = 6\pi\eta R$ with water viscosity $\eta = 10^{-3} Pa \cdot s$. For the ratio γ_y/m_y we thus obtain, assuming a typical radius $R = 1\mu m$, the value $\gamma_y/m_y = 4 \cdot 10^6 s^{-1}$. We note that the radius R of course includes half of the linker that connects the active particles to the central tracer bead, which explains why we use a rather large value for R in our simple estimate. In terms of the dissipation, our result for γ_y/m_y means that in order to reach a non-equilibrium parameter of $\alpha = 1$, Eq. (33) predicts that we need to inject a power of $P = I = 4 \cdot 10^6 k_B T$ per second; this is quite enormous, considering that typical biological motors consume of the order of 100 ATP per second and that the excess free energy of an ATP molecule is about 30 $k_B T$ at physiological conditions [42]. In the experiment shown in Fig. 2, most likely many motors act in parallel on one active unit, which raises the injected power proportionally.

We finally discuss the time scale τ defined in Eq. (30) and that appears in the Lorentz form Eq. (29). Assuming the harmonic coupling potential between active particles and tracer bead to arise from the perpendicular bending of a semi-flexible filament, the harmonic strength is $K \simeq k_B T \ell_P / L^3$ [43], where L denotes the filament length and ℓ_P the persistence length. For the friction coefficient we again assume $\gamma_y \simeq \gamma \simeq 6\pi\eta R$. Choosing all length scales to be of the order of a micrometer, $\ell_P \simeq L \simeq R \simeq 1\mu m$, we obtain from Eq. (30) for the time scale $\tau \simeq 5/\sqrt{n}$ s. The effective time scale thus depends weakly on n, the number of active units that are coupled to the tracer bead, and should be of the order of a second, in agreement with the fit to the experimental data in Fig. 2. We conclude that the fit parameters extracted in Fig. 2 make sense when interpreted physically. In future experimental studies it will be interesting to see how α and τ change when experimental parameters such as ATP concentration, motor and filament density are varied.

CONCLUSION

We have introduced an exactly solvable, Hamiltonian-based many-particle model that accounts for non-equilibrium stochastic driving as well as friction dissipation. On the one hand, by mapping onto a Fokker-Planck equation and solving the stationary distribution in closed form, we characterize the departure from equilibrium by comparison with the Boltzmann distribution. On the other hand, the exact solution of the conjugated Langevin equation allows us to derive a generalized non-equilibrium fluctuation-dissipation relation and thereby to characterize deviations from equilibrium by comparison with the standard equilibrium FDT. Both the stationary distribution as well as the fluctuation-dissipation relation indicate departures from equilibrium as soon as the non-equilibrium parameter α is non-zero, thus these two fundamental indicators of non-equilibrium behavior

are coupled to each other.

We characterize departures from the equilibrium FDT by the experimentally measurable spectral function $\Xi(\omega)$, defined in Eq. (26), which has Lorentz form in the limit of many active particles, as seen in Eq. (29), in excellent agreement with experimental measurements on active filamentous networks, as shown in Fig. 2. $\Xi(\omega)$ depends on the coupling between active particles and tracer bead as well as on the non-equilibrium driving strength, it thus offers a spectral fingerprint of non-equilibrium systems. The non-equilibrium fluctation-dissipation relation Eq. (26) can obviously be interpreted in terms of a frequency-dependent effective temperature, defined by

$$k_B T_{\text{eff}} \equiv k_B T \left(1 + \Xi(\omega)\right), \tag{34}$$

by which the standard equilibrium FDT Eq.(24) would be reinstalled by simply using $k_B T_{\text{eff}}$ instead of $k_B T$. However, this fix falls short of describing the non-equilibrium system in its entirety. This follows from the fact that the non-equilibrium stationary distribution does not only differ from the Boltzmann distribution by a factor in the exponential, which would amount to an effective temperature, but rather shows a fundamentally different symmetry. This can not be explained by an effective scalar temperature, irregardless of its definition. Even if we would introduce effective temperatures that are different for each entry in the covariance matrix, the effective temperatures defined by the non-equilibrium stationary distribution would have to be different from the effective temperature defined by the generalized fluctuation-dissipation relation, as a comparison of the result for the expectation value for $\langle x^2 \rangle$ in Eq. (15) and the spectral function in Eq.(29) shows. Thus we conclude that the concept of an effective temperature, defined by the non-equilibrium fluctuation-dissipation relation, fails to describe the stationary non-equilibrium distribution and thus has to be rejected as a general concept to characterize non-equilibrium systems.

Our model is based on a harmonic Hamiltonian, given in Eq.(1). The generalization to the most general quadratic Hamiltonian with different coupling constants between the active particles and the tracer bead is straightforward but does not change the resulting physics. Non-linear coupling terms are much more difficult to include. However, we note that our harmonic Hamiltonian can be derived from more general non-linear models by a saddle-point analysis in terms of suitably defined coordinates, so we argue that to leading order in a systematic saddle-point expansion, our model results apply to a wide class of more complicated non-linear models.

Useful discussions with A. Mielke are acknowledged. We acknowledge the DFG for funding via the SFB 1114.

[1] C. Bechinger, R. Di Leonardo, H. Löwen, C. Reichardt, G. Volpe, and G. Volpe, Rev. Mod. Phys. **88**, 045006 (2016).
[2] S. Ramaswamy, Annu. Rev. Condens. Matter Phys. **1**, 323 (2010).
[3] S. Katz, J. L. Lebowitz, and H. Spohn, Phys. Rev. B **28**, 1655 (1983).
[4] J. Krug, Phys. Rev. Lett. **67**, 1882 (1991).
[5] B. Schmittmann and R. K. P. Zia, Phys. Rep. **301**, 45 (1998).
[6] J. Dzubiella, G. P. Hoffmann, and H. Löwen, Phys. Rev. E **65**, 021402 (2002).
[7] R. R. Netz, Europhys. Lett. **63**, 616 (2003).
[8] N. Kumar, H. Soni, S. Ramaswamy, and A. Sood, Nature Communications **5**, 4688 (2014).
[9] E. Bertin, M. Droz, and G. Grégoire, Phys. Rev. E **74**, 022101 (2006).
[10] I. Theurkauff, C. Cottin-Bizonne, J. Palacci, C. Ybert, and L. Bocquet, Phys. Rev. Lett. **108**, 268303 (2012).
[11] R. Golestanian, Phys. Rev. Lett. **108**, 038303 (2012).
[12] T. Speck, J. Bialke, A. M. Menzel, and H. Löwen, Phys. Rev. Lett. **112**, 218304 (2014).
[13] F. Ginot, I. Theurkauff, D. Levis, C. Ybert, L. Bocquet, L. Berthier, and C. Cottin-Bizonne, Phys. Rev. X **5**, 011004 (2015).
[14] S. N. Weber, C. A. Weber, and E. Frey, Phys. Rev. Lett. **116**, 058301 (2016).
[15] D. Helbing, Rev. Mod. Phys. **73**, 1067 (2001).
[16] A. Sokolov, I. S. Aranson, J. O. Kessler, and R. E. Goldstein, Phys. Rev. Lett. **98**, 158102 (2007).
[17] R. Suzuki and A. R. Bausch, Nature Communications **8**, 41 (2017).
[18] C. W. Wolgemuth, T. R. Powers, and R. E. Goldstein, Phys. Rev. Lett. **84**, 1623 (2000).
[19] H. Wada and R. R. Netz, Europhys. Lett. **87**, 38001 (2009).
[20] S. R. de Groot and P. Mazur, *Non-Equilibrium Thermodynamics* (North-Holland Pub. Co., Amsterdam, 1962).
[21] G. S. Agarwal, Z. Physik **252**, 25 (1972).
[22] P. C. Hohenberg and B. I. Shraiman, Physica D **37**, 109 (1989).
[23] L. F. Cugliandolo, J. Kurchan, and L. Peliti, Phys. Rev. E **55**, 3898 (1997).
[24] T. Speck and U. Seifert, Europhys. Lett. **74**, 391 (2006).
[25] N. Xu and C. S. O'Hern, Phys. Rev. Lett. **94**, 055701 (2005).
[26] M. Krüger and M. Fuchs, Phys. Rev. Lett. **102**, 135701 (2009).
[27] T. Harada and S. Sasa, Phys. Rev. Lett. **95**, 130602 (2005).
[28] J. Prost, J.-F. Joanna, and J. M. R. Parrondo, Phys. Rev. Lett. **103**, 090601 (2009).
[29] M. Baiesi, C. Maes, and B. Wynants, Phys. Rev. Lett. **103**, 010602 (2009).
[30] U. Seifert and T. Speck, Europhys. Lett. **89**, 10007 (2010).
[31] S. Jabbari-Farouji, D. Mizuno, D. Derks, G. H. Wegdam, F. C. MacKintosh, C. F. Schmidt, and D. Bonn, Europhysics Letters **84**, 20006 (2008).
[32] J. R. KGomez-Solano, A. Petrosyan, S. Ciliberto, R. Chetrite, and K. Gawedski, Phys. Rev. Lett. **103**,

040601 (2009).
[33] J. Mehl, V. Blackly, U. Seifert, and C. Bechinger, Phys. Rev. E **82**, 032401 (2010).
[34] P. Martin, A. J. Hudspeth, and F. Jülicher, Proc. Nat. Acad. Sci. USA **98**, 14380 (2001).
[35] L. Dinis, P. Martin, J. Barral, J. Prost, and J.-F. Joanny, Phys. Rev. Lett. **109**, 160602 (2012).
[36] D. Mizuno, C. Tardin, C. F. Schmidt, and F. C. MacKintosh, Science **315**, 370 (2007).
[37] D. Mizuno, D. A. Head, F. C. MacKintosh, and C. F. Schmidt, Macromolecules **41**, 7194 (2008).
[38] M. Guo, A. J. Ehrlicher, M. H. Jensen, M. Renz, J. R. Moore, R. D. Goldman, J. Lippincott-Schwartz, F. C. MacKintosh, and D. A. Weitz, Cell **158**, 822 (2014).
[39] R. Zwanzig, J. Stat. Phys. **9**, 215 (1973).
[40] A. O. Caldeira and A. J. Leggett, Phys. Rev. Lett. **46**, 211 (1981).
[41] H. Risken, *The Fokker-Planck Equation* (Springer, Berlin, 1984).
[42] J. C. Cochran, Biophys. Rev. **7**, 269 (2015).
[43] T. Odijk, Macromolecules **16**, 1340 (1983).